ELSEVIER

Journal of Molecular Catalysis A: Chemical 152 (2000) 121–132

JOURNAL OF MOLECULAR CATALYSIS A: CHEMICAL

www.elsevier.com/locate/molcata

Catalytic decomposition of formic acid on oxide catalysts III. IOM model approach to bimolecular mechanism

Marek A. Borowiak [a], Michał H. Jamróz [a], Ragnar Larsson [b,*]

[a] *Industrial Chemistry Research Institute, Warsaw, Poland*

[b] *Group of Catalysis Research / Chemical Engineering II, Chemical Center, University of Lund, PO Box 124, 22100 Lund, Sweden*

Received 6 January 1999; accepted 17 June 1999

Abstract

In our previous paper [M.A. Borowiak, M.H. Jamróz, R. Larsson, J. Mol. Catal. A: Chem., 139 (1999) 97], an impulse-oscillation model (IOM) was used for a time description of catalytic acts in the reactions of catalytic decomposition of formic acid on oxide catalysts for unimolecular mechanism. In this paper the bimolecular mechanism were modelled for the same reactions. The results of IOM calculation show the increase of the selectivity of choice of the dehydrogenation path, in comparison to the unimolecular mechanism. The highest increase is for monodentate or bridged forms of adsorbed formate ions (the selectivity 60% in comparison to 42% for the unimolecular mechanism). The OCO bending mode in formate and the O–H surface stretching modes are not so important in the bimolecular mechanism as in unimolecular one. The conclusion can be explained from the point of view of the postulated [H. Onishi, T. Aruga, Y. Iwasawa, J. Am. Chem. Soc. 115 (1993) 10460; H. Onishi, T. Aruga, Y. Iwasawa, J. Catal. 146 (1994) 557; H. Onishi, Y. Iwasawa, Chem. Phys. Lett. 226 (1994) 111; Y. Iwasawa, Stud. Surf. Sci. Catal. 101 (1996) 21] mechanism which does not need strong deformation of OCO bond system and used as a source of acid proton from formic acid and not from surface hydroxyl group on catalyst. The best ranges of wavenumbers for the considered in IOM modes for the dehydrogenation reaction are proposed.

Keywords: Catalytic decomposition; Formic acid; Oxide catalysts

1. Introduction

One goal of recent studies on catalytic decomposition of formic acid on model works is to find the most selective catalyst for the dehydrogenation. To achieve this goal, one can try to understand the chemistry of a particular oxide having a variety of surface sites. However, the chemistry of the surface species appears to be very complex [1] because of a variety of products observed in experiments with different oxides and for different conditions. On the other hand, there are experimental evidence that in particular conditions, high selectivity of one from the two dominant reactions — dehydrogenation or dehydration ones — can be achieved [2–5]. Therefore, another possibility is to look for appropriate conditions for the dehydrogenation reaction to occur at molecular level. Switchover of reaction paths in such selective decomposition is postulated. For the dehydra-

* Corresponding author. Tel.: +46-46-108-113; fax: +46-46-104-439; E-mail: ragnar.larsson@inorgk1.lu.se

1381-1169/00/$ - see front matter
PII: S1381-1169(99)00271-X

tion reaction, the unimolecular decomposition of formates at the surface is rate controlling. Below 500 K, the catalytic dehydrogenation reaction is suggested to proceed as a bimolecular process of a formate ion adsorbed on TiO_2 and formic acid molecule from gas phase.

In our recent paper [6] using the selective energy transfer (SET) model [7], it was found that for the dehydration reaction the asymmetric stretching O–C–O mode while for the dehydrogenation reaction the OCO in plane bending mode are those which must be excited for the reactions to occur. In our previous paper [8], results of modelling the same reactions with the impulse-oscillation model (IOM) showed that the most important modes for the dehydrogenation reaction are the OCO bending mode in the formate and the O–H stretching mode on catalyst surface while for the dehydration reaction — the asymmetric stretching mode OCO in the adsorbed formate and the metal-oxide stretching mode on oxide catalysts. The best ranges of wavenumbers of vibrators taken into account in the model IOM for the dehydrogenation reaction were proposed.

In both our papers [6,8], the unimolecular mechanism of the decomposition reactions was considered. In the present paper, the postulated [2–5] bimolecular mechanism is considered from the point of view of the IOM model.

2. Methods

The search for the best conditions at molecular level for selective occurring of the dehydrogenation reaction was based on a concept of elementary catalytic system [9–16]. The concept combined together spatial-, energetistic- and time-aspects of catalysis. In particular, time conditions of a catalytic act are considered by the IOM model described in our previous papers [8–16]. In this approach, chosen vibrational modes of the reacting system (i.e., molecule of reactant and catalytic center) are considered to be the primary molecular parameters describing the modelling system. The model is based on a set of equations connecting the wavenumbers of the considered modes with discrete moments of simultaneous appearance (named synchronization time) of such favourable distributions of electron density in the reactant and in the catalytic center that the reaction can occur. The number of equations is equal to the number of chosen vibrational modes. Choice of the important modes results from an analysis of assumed mechanism of the reaction. The model calculates possible wavenumber range for each of the mode, within which the synchronization can be reached during the vibrations. In calculation wide ranges are used — expanded to lower and higher wavenumbers in comparison to appropriate experimental ranges — in order to predict what different catalysts can be used for the considered reaction.

Calculation of the IOM are computed on PC Pentium using our program IOMOS [17]. The resulted set of wavenumber ranges for the chosen vibrational modes is used as input data in program IOMAB [16] to determine a selectivity of choice of one way from two possible (A and B) paths. The program IOMAB finds subsets of the ranges where the synchronization for only one way is possible (A or B) and the subsets where synchronization for both paths is possible.In the later case, IOMAB distinguishes a case when synchronization time for the A path is shorter than for the path B (AB case) and a case when shorter is the time for path B (BA case). The selectivity of choice of the path A is calculated in the program IOMAB from the following formula:

$$\mathrm{Sa} = (A + AB + BA)100 \Big/ [A + B + 2(AB + BA)]$$

where A, B, AB, BA are sums (in wavenumbers) of ranges where the above described cases of synchronization are possible.

3. Results and discussion

3.1. Model of the reaction

Three different forms of adsorbed formate ion, namely, monodentate, bidentate and bridged [18] were taken into account in the model. For each of the form, two reaction paths were considered. The dehydrogenation path was named path A and the dehydration path was named path B.

According to the mechanism proposed in the papers [2–5] for the bimolecular dehydrogenation reaction the lateral coulombic (acid–base) interaction between $H^{\delta-}$ of $HCOO_s$ (adsorbed on the TiO_2 surface) and H^+ of HCOOH is more important than the vertical coulombic (acid–base) interaction between $HCOO_s$ and Ti^{4+}. Formate ions on TiO_2 (110) form a monolayer ordered in a (2*1) periodicity. The C–H bond of a formate is normal to the surface, while the O–C–O plane is parallel to the [001] axis. According to the cited authors, it is reasonable that the formates are adsorbed on TiO_2 (110) in a bridge form rather than bidentate or monodentate forms.

A set of 13 vibrational modes was taken into account in the IOM model. The six internal modes of formate ion adsorbed on the surface, the five modes in a molecule of formic acid interacting by two hydrogen bonds with the formate ion, surface OH group and the bonds between oxygen in formate and metal as well as metal–oxygen surface vibrational mode constitute the set.

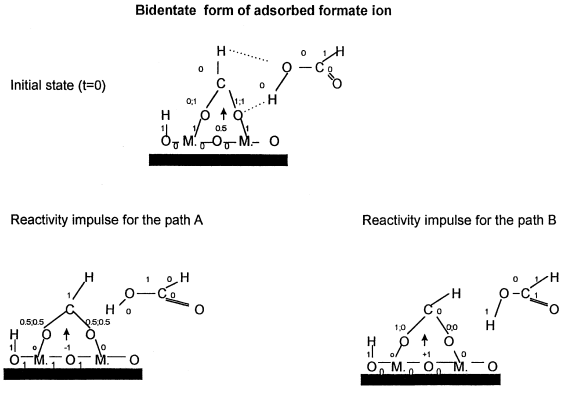

Fig. 1. Scheme of the initial state and the reactivity impulses for bidentate form of adsorbed formate ion.

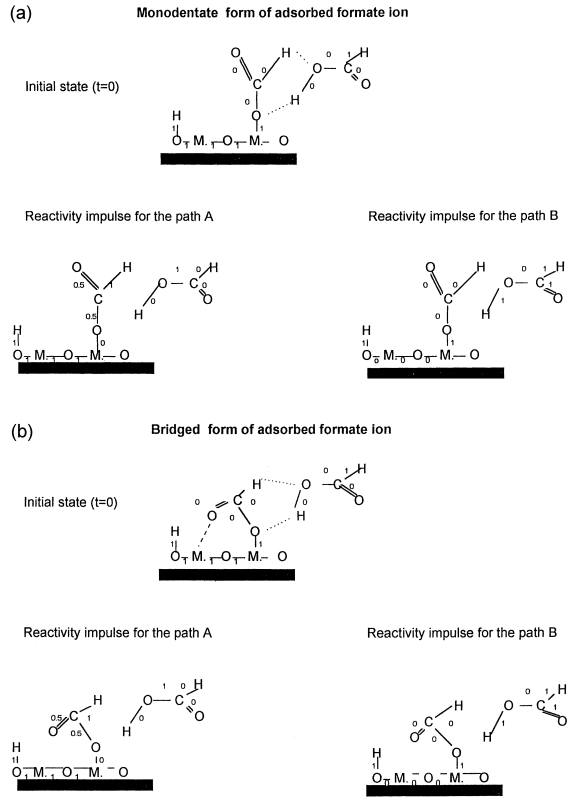

Fig. 2. Scheme of the initial states and the reactivity impulses for monodentate and bridged forms of adsorbed formate ion.

As the initial state ($t = 0$, i.e., the start of measure of time in the model) a moment when the bonds v6 (CO–M.) the v7 (O–H) and the hydrogen bonds have been just formed (therefore, the momentary lengths is assumed in the notation of IOM as 1 — i.e., the longest — see Fig. 1). At that moment, the electron density on the hydrogen in formate and on the acid hydrogen in formic acid are assumed to be the lowest (bond v4 (H–C stretch) and v13 (HCOO–H stretch) at momentary states 0). The lowest electron density on metal (v8 O–M. is 0) is assumed for the bidentate form of formate adsorption (Fig. 1) while for the monodentate and bridged forms — the highest one (Fig. 2). It

means an assumption that the bidentate form is stronger adsorbed then the later forms. Assumption that both formate and formic acid are not deformed is made (all bending modes are at the equilibrium momentary state) for bidentate case while for the monodentate and bridged case, the HCO in formate and OCO in formic acid angles are as small as possible, and the OCO angle in formate is as large as possible.

The reactivity impulse of the formate ion for the path A (dehydrogenation) is defined based on the assumptions of the above-mentioned importance of the negative partial charge on hydrogen atom of formate [2–5] and of a symmetry of OCO bonds while for the path B (dehydration) — the assumption of asymmetry of the bonds system is made. The need of different partial charges on metal for the two paths is taken into account, as well as appropriate deformations of the formates and the acid molecule (Figs. 1 and 2).

In Table 1, the definition of assumed initial states ($t = 0$) for the three adsorbed formate ions and definitions of the reactivity impulses for the two paths are presented.

In order to determine the time of first appearance of the desired distribution of the partial charges in each of the 13 modes taken into account in this model, one has to note that the momentary state 0.5 (equilibrium length of bond) appears two times during one full vibration. One moment is when the vibration is during expansion (let this phase be marked R), the second — during contraction (the phase K). In full analogy, bending motion can be described if at the initial state, it is at the equilibrium state (0.5) and, during the expansion (the R phase of motion), is increasing the angle to maximum (-1), or, during the contraction (the K phase), is decreasing the angle to minimum ($+1$). In this IOM model application (see Table 1), there are three bending modes: v3 (OCO in formate); v5 (HCO in formate) and v11 (OCO in HCOOH) at the equilibrium state (0.5) in the bidentate adsorbed formate. The eight combinations of the phases at the initial state were taken into account in the calculation. Each combination is assigned in a form *XXX*, where $X = \mathrm{R}$ or K and order in the form is v3; v5; v11. Thus, the form RKR means that v3 is in the R phase,

Table 1
Definition of the initial states ($t = 0$) and reactivity impulses for the dehydrogenation (A) and the dehydration (B) reactions -1; 0.5; $+1$ for the bending modes mean the largest, equilibrium and smalest angle, respectively during the bending motion.

Modes	Monodentate			Bidentate			Bridged		
	$t = 0$	A	B	$t = 0$	A	B	$t = 0$	A	B
V1 OCO asymmetric formate				0; 1	0.5; 0.5	1; 0			
V1 C–O formate	0	0.5	0				0	0.5	0
V2 OCO symmetric formate				1	0.5	0			
V2 C = O formate	0	0.5	0				0	0.5	0
V3 OCO bending formate	-1	-1	$+1$	0.5	-1	$+1$	-1	-1	$+1$
V4 H–C stretching formate	0	1	0	0	1	0	0	1	0
V5 HCO bending formate	$+1$	$+1$	$+1$	0.5	$+1$	$+1$	$+1$	$+1$	$+1$
V6 CO–M.	1	0	1	1	0	1	1	0	1
V7 O–H stretching surface	1	1	1	1	1	1	1	1	1
V8 O–M.	1	1	0	0	1	0	1	1	0
V9 OC–O stretching acid	0	1	0	0	1	0	0	1	0
V10 OC = O stretching acid	0	0	1	0	0	1	0	0	1
V11 OCO bending acid	$+1$	-1	$+1$	0.5	-1	$+1$	$+1$	-1	$+1$
V12 H–COOH stretching	1	0	1	1	0	1	1	0	1
V13 HCOO–H stretching	0	0	1	0	0	1	0	0	1

Table 2
Ranges (in wavenumbers) of modes used in the IOM calculation

Modes	Wavenumbers (cm^{-1}) ranges for	
	Bidentate	Monodentate and bridged
V1 OCO asymmetric formate	1650–1500	
V1 C–O formate		1400–1200
V2 OCO symmetric formate	1400–1300	
V2 C = O formate		1620–1500
V3 OCO bending formate	900–700	900–700
V4 H–C stretching formate	2950–2820	2950–2820
V5 HCO bending formate	1100–1005	1100–1005
V6 CO–M.	1200–1080	1200–1080
V7 O–H stretching surface	3500–3200	3500–3200
V8 O–M.	850–350	850–350
V9 OC–O stretching acid	1300–1100	1300–1100
V10 OC = O stretching acid	1780–1600	1780–1600
V11 OCO bending acid	720–610	720–610
V12 H–COOH	2980–2900	2980–2900
V13 HCOO–H	3500–3100	3500–3100

v5 — in the K phase and v11 — in the R phase.

The full IOM applications are presented in Appendix A. The ranges of wavenumbers used in calculation are presented in Table 2.

3.2. Selectivity to the dehydrogenation or to the dehydration reaction

The selectivities toward the path A (dehydrogenation) for each of modes and of the calculated cases are presented in Fig. 3.

For the cases when the formate ion is adsorbed as monodentate or bridged, all the mode selectivities are greater than 50%, i.e., the dehydrogenation reaction is preferred. The most important modes for the selectivity of choice of the reaction are the v1 (C–O stretching mode in formate) (the selectivity 71%) and the v11 (OCO bending mode in formic acid)(70%). The other important modes are the v8 (O–M.) stretching mode on the catalyst surface — 67%, the v3 (OCO) bending mode in formate — 65%, the v2 (C=O) in formate — 63% and the v5 (HCO)

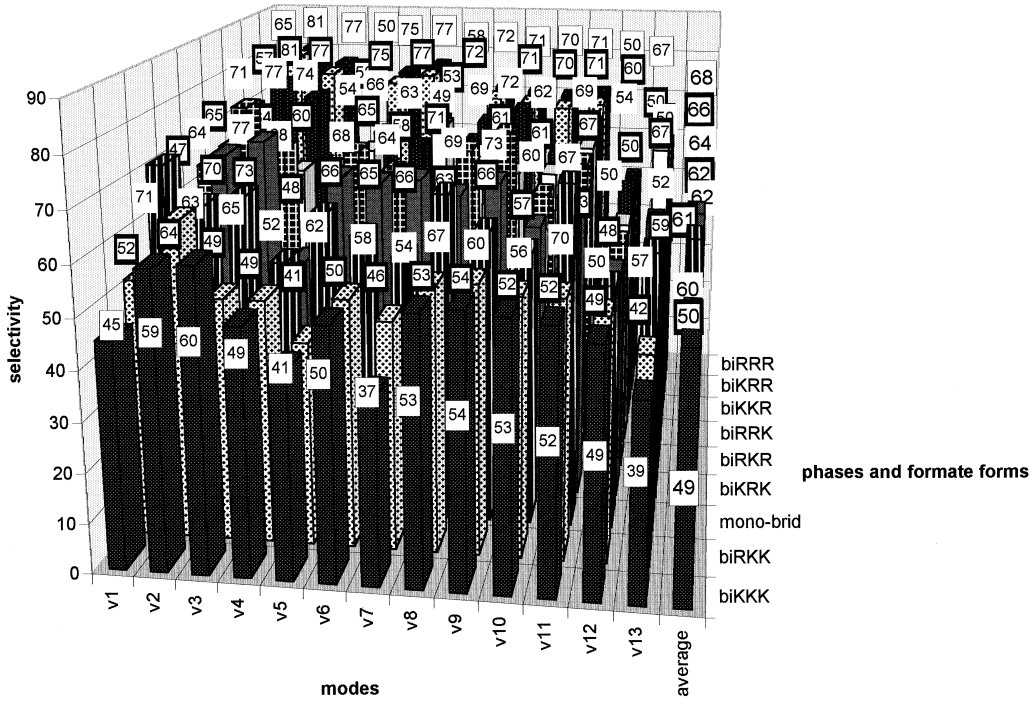

Fig. 3. Selectivity of choice of the dehydrogenation reaction. Monodentate and bridged forms of adsorbed on catalyst surface formate ions are signed as ''mono-brid'', and ''biRRR'' means the bidentate form and the combination RRR in the initial state (see text).

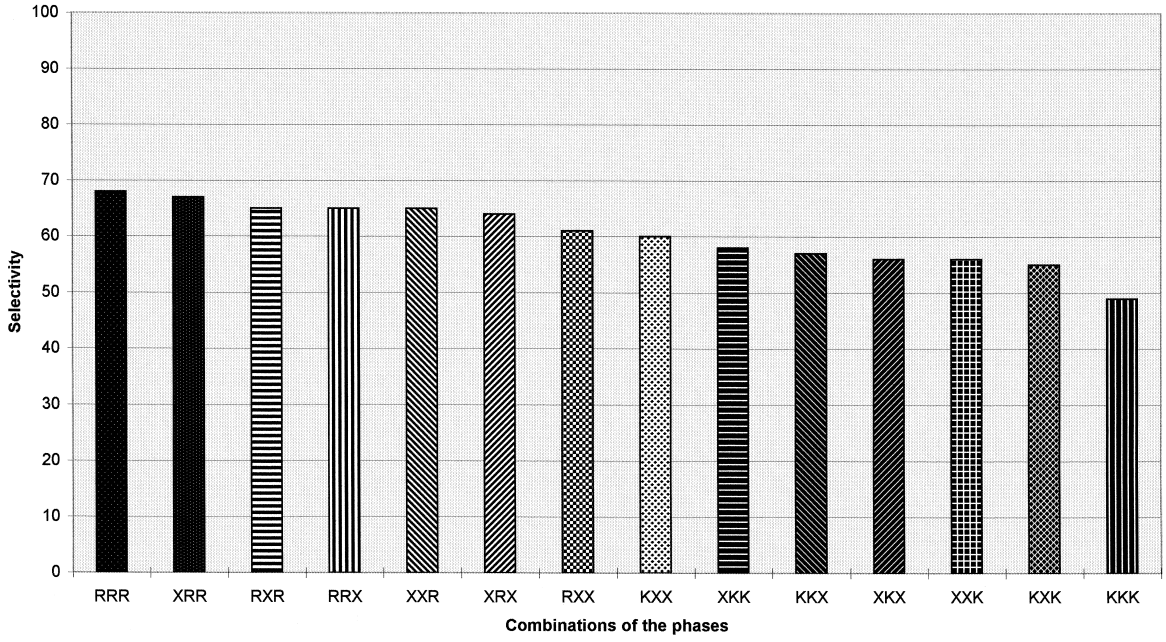

Fig. 4. Averaged selectivities for the dehydrogenation reaction (bidentate). The combination e.g., *XX*R = RRR, RKR, KRR, KKR (*X* = R or K). Selectivity *XX*R is averaged selectivities of all the above mentioned combinations.

bending mode in formate — 62%. The less important mode is v12 (H-COOH) — 50%. The average for all of the modes selectivity is 60%.

For the case of bidentate formate ion adsorbed on the catalyst oxide surface, the selectivity depends on combination of the phases and

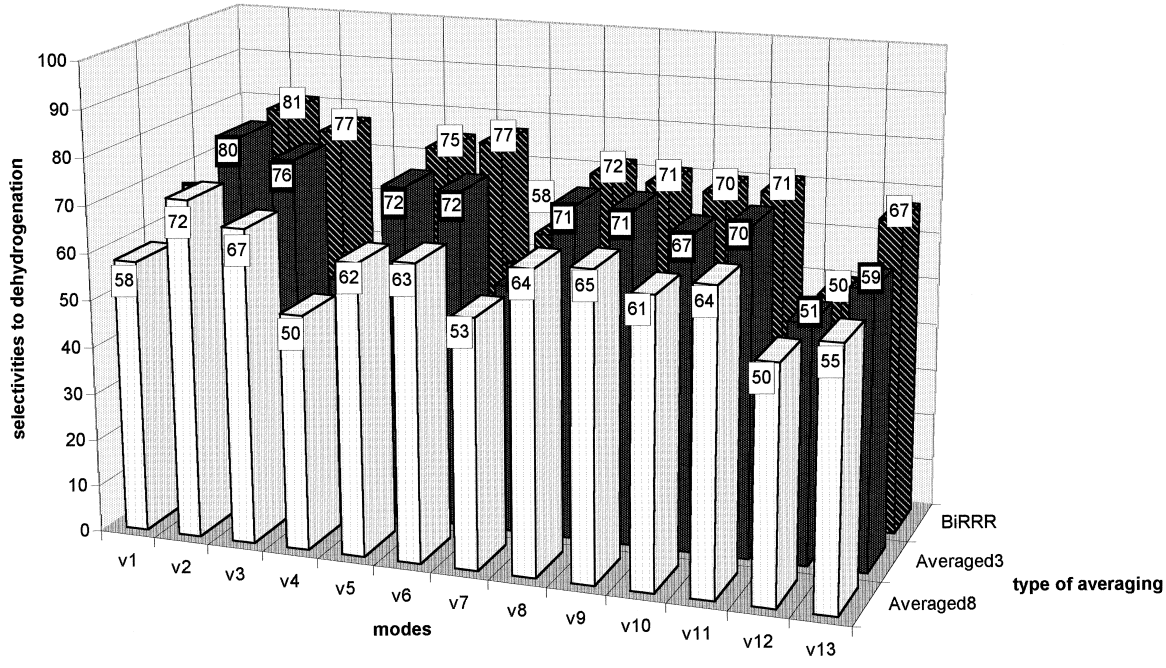

Fig. 5. Bidentate formate: averaged selectivity for all of the combinations (‘‘averaged8’’), averaged for the three highest selectivities for the combinations RRR, KRR, KKR (‘‘averaged3’’) and for the RRR combination.

is highest for the combination RRR (68%) and lowest for the KKK combination (49%). The RRR combination of phases represents the initial situation when all of the bending modes (v3 — OCO; v5 —HCO in formate and v11 — OCO in formic acid — see Table 1) are at state 0.5 and during expansion, the KKK combination — when the abovementioned bending modes are, during contraction.

In Fig. 4, a more detailed analysis of the influence of the combinations of phases in the bidentate case is presented. The symbol *X* means R or K, e.g., RR*X* means the RRR and RRK combinations. The results presented in this figure show that, generally, expansion of the bending modes provides for the dehydrogenation reaction.

In Fig. 5, selectivities to the reaction is presented. Three different values for each of the modes are calculated. The average for all of the combinations (''averaged8''), the averaged for the combinations RRR; KRR and KKR which have the highest selectivities (''averaged3'') and the selectivities for the RRR combination (''bi-RRR''). In all of the calculations, the most important modes are v2 (OCO) symmetric stretching mode in formate (72%; 80%; 81%, respectively) and v3 (OCO) bending mode in formate (67%; 76%; 77%, respectively). Also, the less important modes are the same for all of the calculations, namely, the v4 (H–C) stretching mode in formate (50%; 51% 50%) and the v12 (H–COOH) (50%; 51%; 50%). For the RRR combination, other important modes are the v5 (HCO) bending in formate (75%), the v8 (O–M.) (72%), the v9 (OC–O) stretching mode in the acid (71%), the v11 (OCO) bending in the acid (71%), the v10 (OC=O) stretching mode in the acid (70%) and v13 (HCOO–H) (67%). For the average of all combinations, other important modes are the v9 (OC–O) in the acid (65%), the v8 (O–M.) and the v11 (OCO) bending in the acid (both 64%). The selectivity 63–61% have the v6 (CO–M.), v5 (HCO) bend-

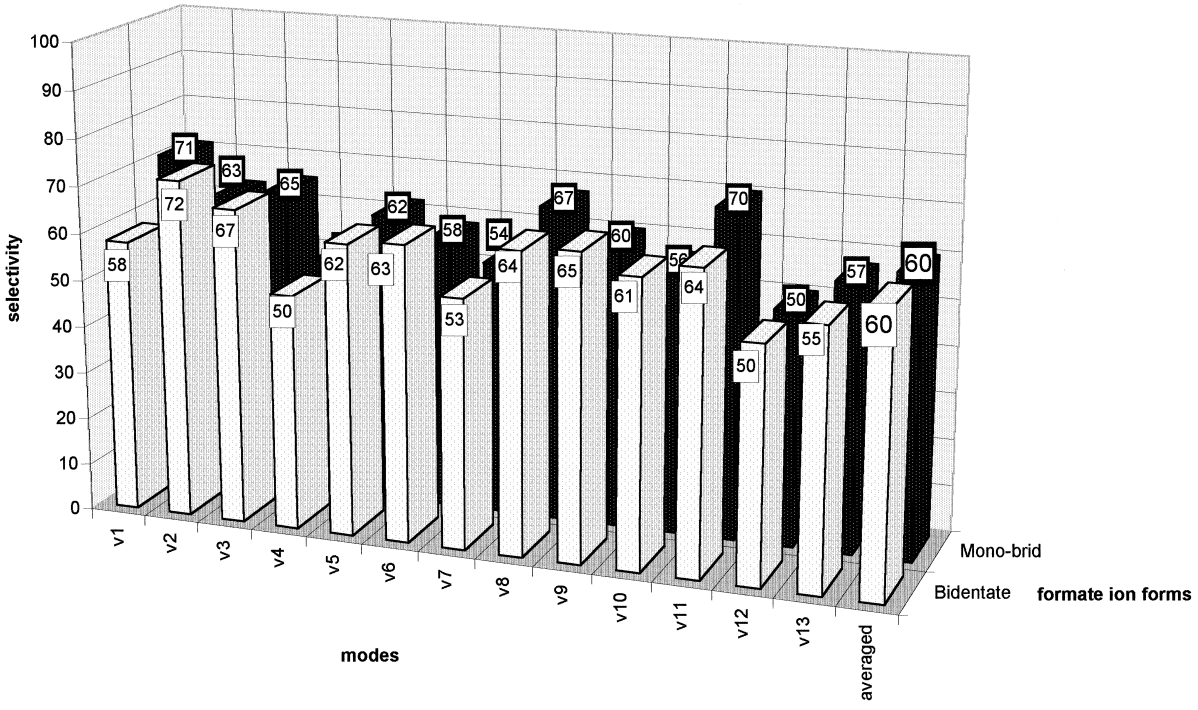

Fig. 6. Selectivity of modes for the dehydrogenation reaction.

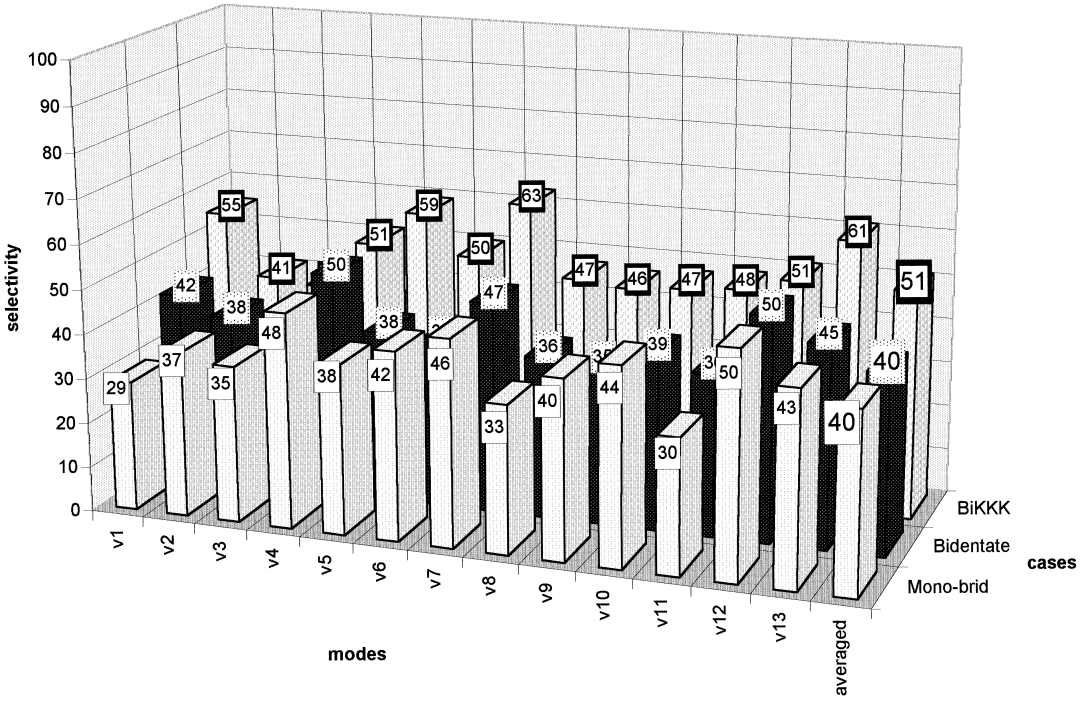

Fig. 7. Selectivity of modes for the dehydration reaction.

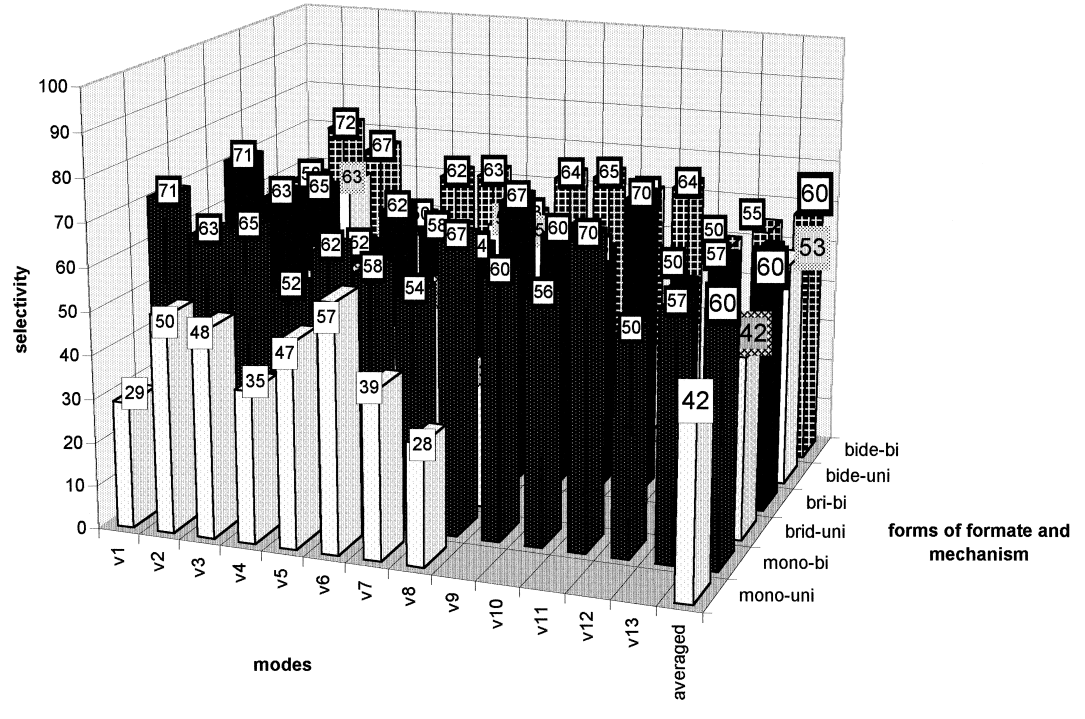

Fig. 8. Comparison of the selectivities for the dehydrogenation reaction between uni- and bimolecular mechanisms.

ing in formate and the v10 (OC=O) stretching in the formic acid.

In Figs. 6 and 7, the selectivities of modes for the dehydrogenation and the dehydration reactions, respectively, are presented.

In Fig. 7, the selectivities for the combinations KKK, where the highest selectivity for dehydration reaction was obtained, are added. For the dehydration reaction in the KKK case of bidentate formate, the most important modes are the O–H (v7) (the selectivity 63%) mode, HCOO–H (v13) mode (61%), HCO (v5) bending mode in formate (59%) and OCO (v1) asymmetric stretching mode in formate (55%). For all of the other cases, the selectivity is lower than 50%. One can say that the most important in cases of monodentate and bridged formate are the following modes: the H–COOH (v12) (the selectivity 50%); the H–C (v4) stretching mode in formate (48%) and O–H surface (v7) stretching mode (46%). The same modes and the decreasing sequence of selectivity values are for averaged selectivity for bidentate.

3.3. Comparison of the selectivity for unimolecular and bimolecular mechanisms

The selectivity for uni- and bimolecular mechanisms for the dehydrogenation (Fig. 8) and for the dehydration reaction (Fig. 9) are compared using the results from this paper and that published in Ref. [8]. The results of IOM calculation based on the mechanism proposed in Refs. [2–5] indicated the increase of the selectivity of choice of the dehydrogenation path in the decomposition reaction of formic acid on oxides metal catalysts. The highest increase is for formate adsorbed as monodentate or bridged forms (selectivity 60% in comparison to 42%

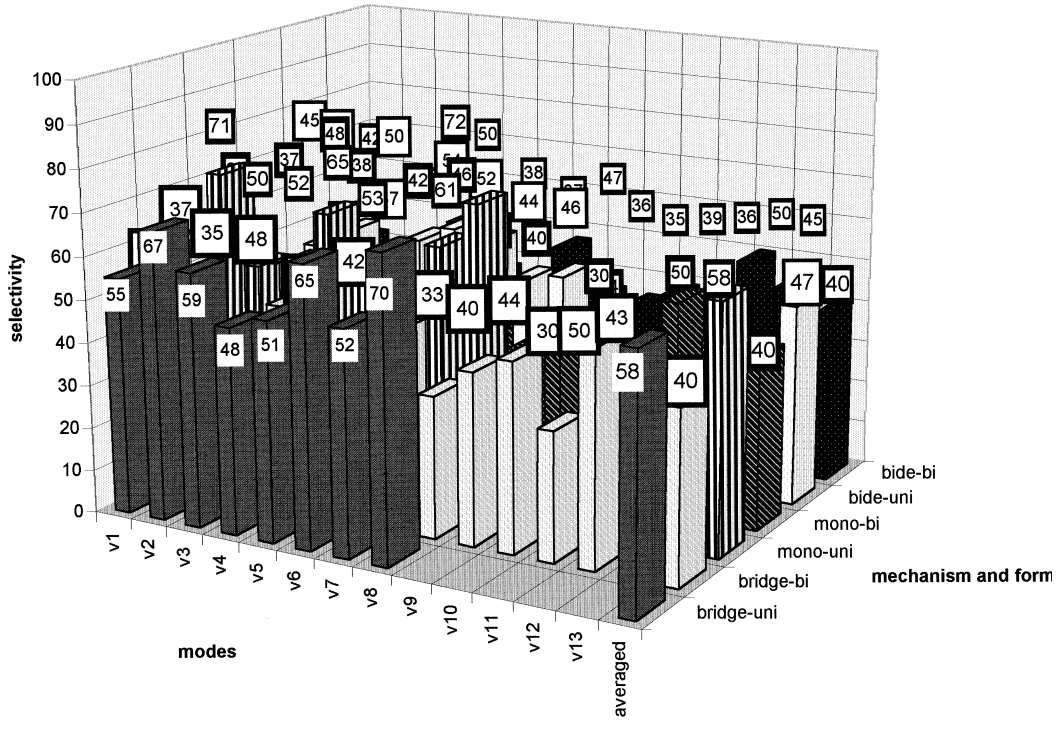

Fig. 9. Comparison of the selectivities for the dehydration reaction between uni- and bimolecular mechanisms.

Table 3
The best ranges for the dehydrogenation reaction

Modes	The best wavenumber (cm^{-1}) ranges for the dehydrogenation reaction for	
	Bidentate	Monodentate and bridged
V1 OCO asymmetric formate	1540–1524	
V1 C–O formate		1400–1398; 1388–1372; 1345–1334; 1317–1301; 1260–1256; 1248–1243; 1233–1223; 1219–1200
V2 OCO symmetric formate	1399–1386; 1324–1300	
V2 C = O formate		1619–1601; 1581–1569; 1566–1556; 1512–1510
V3 OCO bending formate	885–877; 870–857; 794–789; 715–706	900–879; 848–843; 819–804; 786–774; 764–744; 724–714
V4 H–C stretching formate	2950–2900	2858–2851
V5 HCO bending formate	1097–1078; 1042–1039	1096–1088; 1079–1068; 1054–1037; 1008–1005
V6 CO–M.	1135–1107; 1087–1080	1178–1176; 1134–1101;
V7 O–H stretching surface	3443–3423; 3371–3319; 3203–3200	3500–3499; 3394–3370; 3289–3259
V8 O–M.	832–818; 759–748 TiO_2; 681–669 SnO_2; 590–582 V_2O_5(?); 529–521(?); 421–415 CuO; 378–372 ZrO_2(?)	848–843; 819–804; 786–774; 764–744; 724–714 TiO_2; 686–678 SnO_2; 654–645 NiO; 631–627 Cr_2O_3; 611–601 MnO_2(?) 547–544 Cr_2O_3 ; 536–527(?); 524–516 (?); 509–503 CuO; 486–474; 471–470 Fe_2O_3; 458–457 ZnO; 436–434 Cr_2O_3; 412–402; 393–389 MnO_2; 379–377(?); 365–352 ZrO_2
V9 OC–O stretching acid	1286–1246; 1135–1107	1300–1297; 1260–1256; 1252–1243; 1233–1225; 1178–1176; 1134–1100
V10 OC=O stretching acid	1686–1636; 1628–1600	1768–1758; 1701–1667; 1644–1631
V11 OCO bending acid	716–706; 661–650; 643–632	720–704; 695–691; 688–687; 681–668; 658–651; 626–622; 616–612
V12 H–COOH	2950–2900	2979–2900
V13 HCOO–H	3479–3421; 3334–3272; 3171–3123	3471–3434; 3354–3339; 3317–3305; 3229–3176

Appendix A

A.1. The IOM model for bidentate form for the dehydrogenation reaction

Phases	()/v1	()/v2	()/v3	()/v4	()/v5	()/v6	()/v7	()/v8	()/v9	()/v10	()/v11	()/v12	()/v13
RRR	0.25 + 0.5n1	0.25 + 0.5n2	0.25 + n3	0.5 + n4	0.25 + n5	0.5 + n6	0 + n7	0.5 + n8	0.5 + n9	0 + n10	0.25 + n11	0.5 + n12	0 + n13
RRK	0.25 + 0.5n1	0.25 + 0.5n2	0.25 + n3	0.5 + n4	0.25 + n5	0.5 + n6	0 + n7	0.5 + n8	0.5 + n9	0 + n10	0.75 + n11	0.5 + n12	0 + n13
RKR	0.25 + 0.5n1	0.25 + 0.5n2	0.25 + n3	0.5 + n4	0.75 + n5	0.5 + n6	0 + n7	0.5 + n8	0.5 + n9	0 + n10	0.25 + n11	0.5 + n12	0 + n13
KRR	0.25 + 0.5n1	0.25 + 0.5n2	0.75 + n3	0.5 + n4	0.25 + n5	0.5 + n6	0 + n7	0.5 + n8	0.5 + n9	0 + n10	0.25 + n11	0.5 + n12	0 + n13
RKK	0.25 + 0.5n1	0.25 + 0.5n2	0.25 + n3	0.5 + n4	0.75 + n5	0.5 + n6	0 + n7	0.5 + n8	0.5 + n9	0 + n10	0.75 + n11	0.5 + n12	0 + n13
KRK	0.25 + 0.5n1	0.25 + 0.5n2	0.75 + n3	0.5 + n4	0.25 + n5	0.5 + n6	0 + n7	0.5 + n8	0.5 + n9	0 + n10	0.75 + n11	0.5 + n12	0 + n13
KKR	0.25 + 0.5n1	0.25 + 0.5n2	0.75 + n3	0.5 + n4	0.75 + n5	0.5 + n6	0 + n7	0.5 + n8	0.5 + n9	0 + n10	0.25 + n11	0.5 + n12	0 + n13
KKK	0.25 + 0.5n1	0.25 + 0.5n2	0.75 + n3	0.5 + n4	0.75 + n5	0.5 + n6	0 + n7	0.5 + n8	0.5 + n9	0 + n10	0.75 + n11	0.5 + n12	0 + n13

A.2. The IOM model for bidentate form for the dehydration reaction

	()/v1	()/v2	()/v3	()/v4	()/v5	()/v6	()/v7	()/v8	()/v9	()/v10	()/v11	()/v12	()/v13
RRR	0.5 + n1	0.5 + n2	0.75 + n3	0 + n4	0.75 + n5	0 + n6	0 + n7	0 + n8	0 + n9	0.5 + n10	0.75 + n11	0 + n12	0.5 + n13
RRK	0.5 + n1	0.5 + n2	0.75 + n3	0 + n4	0.75 + n5	0 + n6	0 + n7	0 + n8	0 + n9	0.5 + n10	0.25 + n11	0 + n12	0.5 + n13
RKR	0.5 + n1	0.5 + n2	0.75 + n3	0 + n4	0.25 + n5	0 + n6	0 + n7	0 + n8	0 + n9	0.5 + n10	0.75 + n11	0 + n12	0.5 + n13
KRR	0.5 + n1	0.5 + n2	0.25 + n3	0 + n4	0.75 + n5	0 + n6	0 + n7	0 + n8	0 + n9	0.5 + n10	0.75 + n11	0 + n12	0.5 + n13
RKK	0.5 + n1	0.5 + n2	0.75 + n3	0 + n4	0.25 + n5	0 + n6	0 + n7	0 + n8	0 + n9	0.5 + n10	0.25 + n11	0 + n12	0.5 + n13
KRK	0.5 + n1	0.5 + n2	0.25 + n3	0 + n4	0.75 + n5	0 + n6	0 + n7	0 + n8	0 + n9	0.5 + n10	0.25 + n11	0 + n12	0.5 + n13
KKR	0.5 + n1	0.5 + n2	0.25 + n3	0 + n4	0.25 + n5	0 + n6	0 + n7	0 + n8	0 + n9	0.5 + n10	0.75 + n11	0 + n12	0.5 + n13
KKK	0.5 + n1	0.5 + n2	0.25 + n3	0 + n4	0.25 + n5	0 + n6	0 + n7	0 + n8	0 + n9	0.5 + n10	0.25 + n11	0 + n12	0.5 + n13

A.3. The IOM model for monodentate and bridged forms for the dehydrogenation (A) and dehydration (B)

	()/v1	()/v2	()/v3	()/v4	()/v5	()/v6	()/v7	()/v8	()/v9	()/v10	()/v11	()/v12	()/v13
A	0.25 + 0.5n1	0.25 + 0.5n2	0 + n3	0.5 + n4	0 + n5	0.5 + n6	0 + n7	0 + n8	0.5 + n9	0 + n10	0.5 + n11	0.5 + n12	0 + n13
B	0 + n1	0 + n2	0.5 + n3	0 + n4	0 + n5	0 + n6	0 + n7	0.5 + n8	0 + n9	0.5 + n10	0 + n11	0 + n12	0.5 + n13

Program IOMOS is used to solve the parameterized equations: $(w_1 + k_1 * n_1)/\nu 1 = \ldots = (w_8 + k_8 n_8)/\nu 8$, where ν = IR frequencies; n = integer number of vibration cycles; k, w = phase coefficients due to model formalism. ''()'' = $(w_i + k_i * n_i)$.

for the unimolecular mechanism). This result is connected with changes of modes which are most important in the unimolecular reaction. In particular, the OCO bending mode in formate and the O–H surface stretching modes are not such important in the bimolecular mechanism as in unimolecular one. The conclusion can be explained from the point of view of the postulated [2–5] mechanism which does not need big deformation of OCO bond system and used as a source of acid proton from formic acid, and not from surface hydroxyl group on catalyst.

3.4. The best ranges of wavenumbers for dehydrogenation reaction

The best ranges of wavenumbers for the considered modes for the dehydrogenation reaction are presented in Table 3. The assigned metal oxides are proposed based on the spectroscopic data collected in the Davydov book [19].

Acknowledgements

This work is part of a COST project, D3/007/94 ''Modelling of selective energy transfer, spatial and time coherence in catalytic reactions, tested on carbon dioxide reactions''. Polish authors thank K.B.N. for financial support of the COST project by grant no. 3T09B03309.

References

[1] M.A. Henderson, J. Phys. Chem. B 101 (1997) 221.
[2] H. Onishi, T. Aruga, Y. Iwasawa, J. Am. Chem. Soc. 115 (1993) 10460.
[3] H. Onishi, T. Aruga, Y. Iwasawa, J. Catal. 146 (1994) 557.
[4] H. Onishi, Y. Iwasawa, Chem. Phys. Lett. 226 (1994) 111.
[5] Y. Iwasawa, Stud. Surf. Sci. Catal. 101 (1996) 21.
[6] R. Larsson, M.H. Jamróz, M.A. Borowiak, J. Mol. Catal. A: Chem. 129 (1998) 41.
[7] R. Larsson, J. Mol. Catal. 55 (1989) 70.
[8] M.A. Borowiak, M.H. Jamróz, R. Larsson, J. Mol. Catal. A: Chem. 139 (1999) 97.
[9] M.A. Borowiak, ISSOL 86, Berkeley, USA, 1986, Abstr., p. 306.
[10] M.A. Borowiak, in: Prep. Pap. Pres. 196th Am. Chem. Soc. Nat. Meeting, Los Angeles, USA, 33 (4) (1988) 647.
[11] M.A. Borowiak, Biophys. Chem. 32 (1988) 21.
[12] M.A. Borowiak, Introduction to Modelling of Catalytic System, Ossolineum, Wrocław, 1990, in Polish.
[13] M.A. Borowiak, Acta Pharm. Pol.- Drug Res. 48 (3–4) (1991) 75.
[14] M.A. Borowiak, Elementary Catalytic System Model for Rational Design of Catalysts at Atomic/Molecular Levels, Ossolineum, Wrocław, 1991.
[15] M.A. Borowiak, J. Haber, J. Mol. Catal. 82 (1993) 327.
[16] M.A. Borowiak, M.H. Jamróz, Internet J. Chem., http://www.ijc.com/articles/1998v1/17/.
[17] M.H. Jamróz, ICRI Internal Report 1996 unpublished.
[18] P.A. Dilare, J.M. Vohs, J. Phys. Chem. 47 (1993) 12922.
[19] A.A. Davidov, IR Spectroscopy in Oxide Surface Chemistry, Nauka, Novosibirsk, 1984, in Russian.